Pergamon

Available online at www.sciencedirect.com
SCIENCE DIRECT®

Cement and Concrete Research 33 (2003) 1063–1070

CEMENT AND CONCRETE RESEARCH

Pore solution analysis of cement pastes and nanostructural investigations of hydrated C_3S

Josef Tritthart[a,*], Frank Häußler[b]

[a]Technische Versuchs-und Forschungsanstalt Technische Universität Graz (TVFA), A-8010 Graz, Austria
[b]Institut für Gesteinshüttenkunde Montanuniversität Leoben, A-8700 Leoben, Austria

Received 21 August 2001; accepted 2 January 2003

Abstract

Pore solution investigations of cement pastes which had been prepared with the addition of ethanolamine showed that the ethanolamine had not been bound by cement during hydration and remained more or less completely dissolved in the capillary water, which can (theoretically) be expressed. This suggests that no significant binding of ethanolamine had occurred, neither chemically nor by way of adsorption and that the physically bound water (gel water) could not act as a solvent for the ethanolamine. The latter seems to be in contrast to the frost theory according to which a part of the gel water is mobile [M. Setzer, Micro ice lens formation, in: M.J. Setzer (Ed.), Proceedings of the 3rd International Bolomey Workshop "Pore Solution in Hardened Cement Paste", University of Essen, June 1998, AEDIFICATIO Publishers, Freiburg, 2000, pp. 89–112]. This shows that a better understanding of structural details in the nanometer range of hardened cement is necessary. Therefore, small-angle neutron scattering (SANS) experiments were performed to study this part of the structure using C_3S. SANS studies allow a nondestructive description of statistically representative microstructures in the scale range from micrometer to nanometer. In contrast to the established methods for microstructural investigations like MIP or BET, nondried samples can be used. Moreover, the scattering signals can be analyzed in a variety of ways, and therefore, a more detailed insight can be provided into the very complex cement paste microstructure. In this study, the signals were evaluated with respect to the specific inner surface and the particle-size distribution in the investigated nanometer range up to $\sim$100 nm.

Keywords: C_3S; Cement-paste; Binding of ethanolamine; Microstructure; Gel water

1. Introduction

The formation of the hydration products of cement occurs in the liquid phase. As there a chemical equilibrium exists between the pore solution and the solids, every change in the composition of the pore solution, caused, e.g., by the addition of substances and/or environmental influences, can result in a change of the chemical/physical behavior of the hydration products. As many properties of concrete such as strength, permeability, durability, etc. depend mainly on the microstructure of the cement paste, there is a certain link between the pore solution chemistry and the macroscopic properties of the cement paste. It is well known that the latter is strongly influenced by the cement composition and the water/cement value [2]. As the main part of Portland cement clinker consists of C_3S (50–70 mass%) and C_2S ($\sim$20 mass%), these minerals are of particular importance. During hydration, they form the C–S–H phase, which is most important for the macroscopic behavior of the hardened paste (strength, etc.) [3]. Fig. 1 shows exemplarily the morphology of the hydration products obtained by environmental scanning electron microscope (ESEM). From this picture, it seems to be obvious that the microstructure is very complicated and sensitive to invasive preparation procedures.

In the following, experiments are described carried out by (i) pore solution analysis (PSA) and (ii) small-angle neutron scattering (SANS). The latter is a well-known method to study colloidal materials in a nondried state. First, the used methods and experiments are briefly described followed by the results and the discussion. The generally accepted abbreviations of the cement chemistry

* Corresponding author. Tel.: +43-316-873-7158; fax: +43-316-873-7650.
E-mail address: tri@tvfa-tu-graz.ac.at (J. Tritthart).

0008-8846/03/$ – see front matter © 2003 Elsevier Science Ltd. All rights reserved.
doi:10.1016/S0008-8846(03)00011-5

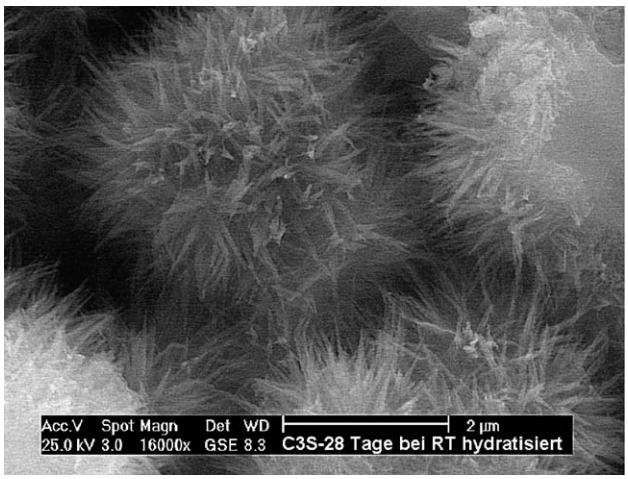

Fig. 1. ESEM-FEG images of hydrating tricalcium silicate (C_3S) 28 days after the onset of hydration at room temperature [B. Möser, FIB Weimar, 1999].

are used, C for CaO, S for SiO_2, H for H_2O, and in analogy D for D_2O.

2. Methods

2.1. Pore solution analysis

Expression of pore solution of cement paste and concrete is relatively often used in research laboratories, e.g., for studying equilibria of substances between the solids and the liquid phase and has been described first by Barneyback and Diamond [4]. The determined concentration of a substance, e.g., of chloride in the pore solution and its known or determined total content, provides the basis to answering fundamental questions, e.g., how much of the substance is free/bound in cement at a certain *w/c* value. The method is primarily interesting in connection with chemical questions but not with structural ones. However, during studies on the binding of an ethanolamine in cements, results were obtained affecting the properties of gel water, and this is why microstructural investigations of the colloidal C–S–H phase were carried out as well.

2.2. Small-angle neutron scattering

SANS experiments deliver a nondestructive description of statistically representative microstructures (nanometer and micrometer scale) in disordered materials. SANS provides average information on an ensemble of scattering objects. The basics of SANS [5–7] and a detailed description of SANS application are given in Refs. [5–11]. The inversion of the scattering pattern to real space cannot yield specific data of individual scattering centers as does a direct imaging method. Therefore, a reciprocal picture of the real world is obtained. Certain models [2,3,12] about the hydrating system are needed for an interpretation of experimental results.

SANS has the following advantages over the conventional methods such as mercury intrusion porosimetry (MIP) [13] and gas sorption (BET) [14].

- Sample preparation as well as the measurement itself does not significantly influence the microstructure. A real picture of the microstructure under given conditions is provided.
- Repeated measurements at the same sample are possible. For example, time-dependent changes in the microstructure during hydration can be investigated.
- Wet samples can be used.

The possibility to use wet samples is a crucial advantage because during drying necessary for MIP and BET, the microstructure is irreversibly changed. The used SANS instrument V4 (Hahn-Meitner Institute [HMI] Berlin, Germany) is sensitive to the size region of about $\sim 10^{-9}$ m to $\sim 4 \times 10^{-7}$ m (nanometer range). The SANS pattern is dominated by the hydration products including portlandite and calcite. The SANS signals of the hydration products are significantly higher than those of the nonhydrated cement [15]. A detailed description of the instrument V4 is given on the internet (http://www.hmi.de/bensc/instrumentation/instrumente/v4).

3. Experimental

PSA studies had been carried out to determine the binding of ethanolamine in cement in the context of a research project on corrosion inhibitors containing amino-alcohols. Three different types of cement from Austrian manufacturers were used: (i) normal Portland cement PZ-375-EZ; this is an OPC which is commercially available and is produced by mixing equal quantities of cement PZ-375 from all Austrian manufacturers; (ii) EPZ; it contains about 30 M% blast furnace slag; (iii) HS-cement; cement with enhanced resistance against sulfate attack (≤ 3 mass% C_3A). The composition of the cements is summarized in Table 1. For sample preparation, the corrosion inhibitor was

Table 1
Composition of the cements (mass%)

	PZ 375 EZ	EPZ	HS-cement
Loss on ignition (1000 °C)	2.6	1.9	1.2
Insoluble residue	0.7	0.6	0.6
SiO_2	19.9	24.7	21.2
Al_2O_3	4.6	7.9	3.2
Fe_2O_3	2.7	1.7	4.8
CaO	61.9	54.1	63.1
MgO	2.4	3.4	1.4
SO_3	2.9	2.6	2.4
Na_2O	0.3	nd	nd
K_2O	1.0	nd	nd
C_3A (Bogue)	nd	nd	0.3
Specific surface (Blaine, m^2/g)	3550	2900	2850

first dissolved in the mixing water, and then the cement was added. The cement pastes, which had been produced by manual mixing with a spoon, were filled into plastic containers with tight caps and rotated until hardening (overnight) to avoid demixing. Until testing, the containers were stored in closed state at 20 °C. The water-to-cement ratio of the samples was 0.6. Some of the pore solution was expressed at a sample age of 28 days. The device that had been used is described in Ref. [16]. The ethanolamine was quantified in the expressed pore solution by ion chromatography.

For the SANS experiments, synthesized cement clinker C_3S (FIB Weimar) was mixed with heavy water (D_2O). The *w/s* value was 0.4 (sample code P6; thickness 0.93 mm) and 0.6 (sample code P13; thickness 0.96 mm). Although the rate of hydration is influenced by D_2O at least during the first days of hydration [17,18], heavy water was used for hydration because of the better signal–noise ratio of the SANS pattern. To make the results comparable and to avoid any misunderstandings with regard to degree of hydration, only D_2O was used.

After mixing, the pastes were put into circular plastic cells (Ø14 mm; thickness ~1 mm). Then the samples were stored for 24 h at 100% relative humidity. Later on, they were stored in desiccators (not containing any drying agent and filled with normal air) at room temperature until required for testing (~1 month). Therefore, carbonation effects to the microstructure cannot be excluded. The influence of carbonation to the SANS pattern is described elsewhere [19]. The objective of these investigations was to discuss results of samples hydrated under technologically representative conditions. Furthermore, C_3S was used as a model substance to study the C–S–H-phases.

4. Results

4.1. PSA

Fig. 2 shows the concentration of ethanolamine in the pore solution of three different cements (*w/c* value 0.6; age of the sample: 28 days) in dependence on the total inhibitor content. The concentrations were highest in PZ 375, followed by HS-cement and EPZ. The concentration of the ethanolamine found in the pore solution was much higher than the concentration in the mixing water so that it was not clear if any of the ethanolamine was bound by cement. Providing a precise answer to this question is not easy. Three types of water are considered to be present in a hydrated cement, namely, (i) chemically bound, (ii) physically bound by adsorption (gel), and (iii) free (capillary) water. At drying, the capillary water and the gel water evaporate so that the amount of chemically bound water can be determined by drying either at elevated temperatures or at room temperature in a vacuum, e.g., over P_2O_5. However, the measuring value depends on the drying

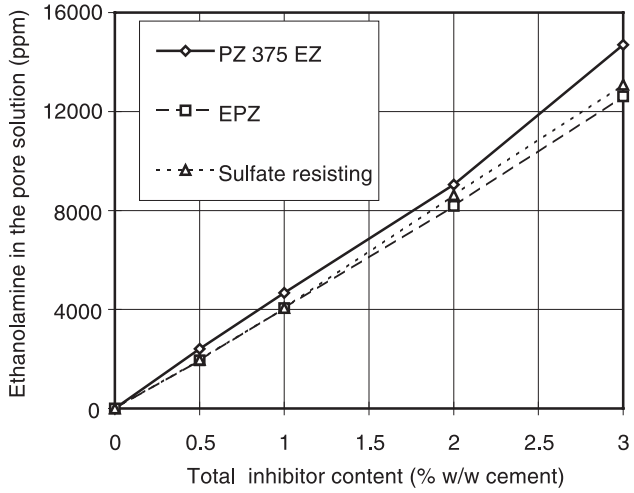

Fig. 2. Concentration of ethanolamine in the pore solution versus total inhibitor content.

conditions so that it is not possible to say if the measured value is "true." It is much more problematic to distinguish between the capillary water and the gel water. According to Powers and Brownyard [20], all evaporable water is in the gel below vapor pressures of 0.3–0.45. However, according to Feldman and Sereda [21], gel pores in the sense of water-filled pores do not exist. Beaudoin and Brown [22] gave an overview of the different models in 1993 according to which the greatest part of the "gel water" must be considered as bound. Although it cannot be excluded that there exists a small part of real pores having dimensions of the gel particles, the major part of the "gel pores" must be considered as a space in the interior of hydration products which can be occupied only by water [22]. However, according to the frost theory, the volume shrinkage of cement paste and concrete at the beginning of the formation of ice within the capillary pores is explained by a movement of gel water out of the gel pores into the capillary pores [1]. This is possible only if the gel water is present in pores (gel pores), and if it is not bound. In recent years, investigations on the mobility of water in hardened cement pastes have been carried out via different methods, such as nuclear magnetic resonance (NMR) [23,24] or quasielastic neutron scattering (QNS) [25,26], which allow to classify the type of water. Their results are not discussed in detail here as it was the intention of the authors to give a rough estimate of how much ethanolamine was bound by the cement only. The approach that was adapted was as follows.

Based on the results of Powers and Brownyard [20], it was assumed that the bound portion of water (bound both chemically and physically) of the paste of a normal Portland cement (consisting mainly of clinker and gypsum only) with a *w/c* ratio of 0.6 can be estimated to lie between about 25 and 30 mass% of the cement mass after 28 days of hydration. The share of capillary water, i.e., the water which theoretically can be expressed, must accordingly have dropped from initially 60% to about 30–35% of the cement

mass during the 28 days of hardening (the mixing water content amounted to between about 170 and 200 mass% of the capillary water in the hardened samples). The concentration of a substance which is not bound by cement must have increased by the same percentage as the content of free water decreased, i.e., its percentage in the expressed pore solution must have been between about 170 and 200 mass% of its concentration in the mixing water. Table 2 shows the changes in concentration of the ethanolamine.

The fact that the rise in concentration in PZ-375-EZ could be explained by the loss of free water caused by hydration indicated that most probably, no ethanolamine was bound at least in this cement. The HS-cement and EPZ either bound small amounts of ethanolamine, or their content of unbound water was still higher after 28 days than in PZ-375-EZ, so that the concentration of ethanolamine was unable to rise to an equally high level. More detailed information cannot be provided yet since the content of unbound water in the samples has not been determined.

Other results of the PZ-375-EZ showed that, as expected, the ethanolamine concentration of the pore water decreased at growing *w/c* value. As regards the increase in concentration in the liquid phase compared to the initial value in the respective mixing water, a calculation was performed analogous to the above one under the assumption that the bound portion of water was between 25 and 30 mass% in all samples irrespective of their different *w/c* values.

The values summarized in Table 3 show that with respect to the concentration of ethanolamine in the pore solution (related to its concentration in the mixing water), the closer to the upper limit of the mixing water content (related to the content of unbound water in the hardened samples), the higher the *w/c* value was; at a *w/c* value of 0.7, it was even slightly above this upper limit. In all likelihood, this is due to the fact that the content of chemically or physically bound water in samples of the same age were, after all, also dependent on the *w/c* ratio; in the sample with a *w/c* value of 0.7, it was apparently already somewhat above the assumed upper limit of 30 mass% of the cement mass. At any rate, these results prove yet again that the ethanolamine remained dissolved in pastes of this cement and was not being bound.

Table 2
Changes in concentration during hardening (calculated value)

	Total inhibitor content (*w/w*-cement)			
	0.5	1.0	2.0	3.0
	Ethanolamine concentration in the pore solution (in percent of its concentration in the mixing water)			
PZ-375-EZ (OPC)	194	188	182	197
(EPZ; ~30% BFS)	157	163	165	169
HS-cement ($\leq$3% C_3A)	135	163	173	175

Table 3
Changes in concentration during hardening (calculated value)

w/c ratio	Mixing water content (in percent of the content of unbound water in the hardened sample)	Ethanolamine concentration in the pore solution (in percent of its concentration in the mixing water)
0.50	200–250	232
0.60	170–200	186
0.70	155–175	177

The fact that the ethanolamine was present in the samples from the very beginning and rose to values which can be explained by the increase in concentration caused by the decrease in the content of free water shows that, obviously, no ethanolamine was present in the so-called gel water, which is considered to be physically bound by adsorption [20] or to be a part of the structure (chemically bound) [21,22]. However, according to the frost theory, the gel water is structured and at least a part of it can move out of the gel pores, and therefore, it cannot be considered as bound in the strict sense of this word. This makes clear that there is a need for a better understanding of the microstructural details of the gel part of cement paste. Conventional methods, such as BET or mercury intrusion measurements, have the disadvantage that dried samples must be used, but the microstructure is irreversibly changed during drying. Although an answer to the question inasmuch as the gel water is mobile could not be anticipated, microstructural investigations into the gel part had been carried out by SANS because this method is particularly suited for investigating cement gel.

4.2. SANS

The scattering curves of two different samples of hydrating C_3S are shown in Fig. 3. The scattering signal after instrumental corrections is given by the macroscopic differential small-angle scattering cross-section $d\Sigma/d\Omega\,(Q)$. Here, Σ is the macroscopic cross-section (the reciprocal value of

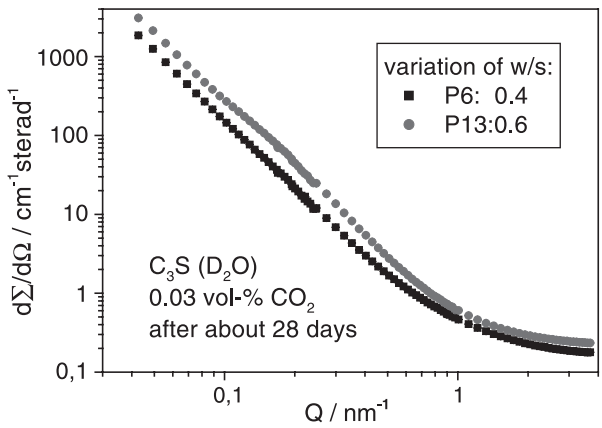

Fig. 3. SANS curves of hydrating C_3S 28 days after the onset of hydration. The two samples are different in the *w/s* value.

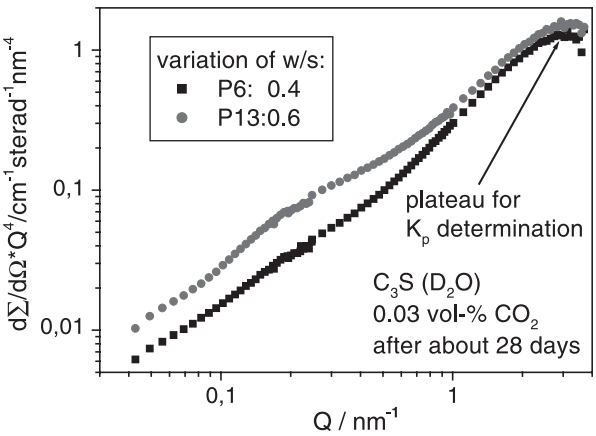

Fig. 4. Porod plot of the scattering curves of Fig. 3 is given. Here a small plateau of a Porod-like behavior is evident.

Σ gives the attenuation of the primary neutron beam by scattering), dΩ is the solid-angle element measured in steradians. The scattering vector Q depends on the scattering angle θ and the neutron wavelength λ. Its magnitude Q describes the deflection of the scattered neutron from the primary beam direction. A detailed description of SANS on hydrating cement paste and an explanation of the quantitative evaluation (formulas) is given, e.g., in Refs. [6,7,27,28]. A scattering curve is a direct measuring result after data treatment which can be discussed qualitatively without any model assumptions or approximations. This is usually the first step in data analysis. Looking at the two curves in Fig. 3, differences in the microstructure of the C_3S samples, which were mixed differently (*w/s* value), are directly visible. The different shape of the curves is an indicator for differences in the resolvable microstructure. The segments of the scattering curves in the region of $Q>1$ nm^{-1}, which corresponds to sizes of some nanometers (<6 nm), are not changed in shape but in intensity [$d\Sigma/d\Omega(Q)$]. This means that the number of small particles (some nanometers) increases with increasing *w/s* value. In contrast, the segments of the two scattering curves in the region $Q<1$ nm^{-1}, which corresponds to sizes of several nanometers (>6 nm), is changed in shape and in intensity. This qualitative result can be explained by a numerical increase of larger particles (several nanometers) with increasing *w/s* value.

The second step in data analysis is the application of different scattering laws based on model assumptions. In this paper, a quantitative interpretation of the qualitatively discussed results should be attempted into two directions, applying well-established procedures for data analysis. Firstly, the specific inner surfaces of both samples P6 and P13 were estimated by means of the Porod law [6,7]. Secondly, the particle-size distribution was determined by an indirect Fourier transformation method [29,30] (here in a size range of about 1–100 nm) to illustrate the scattering results in a way more familiar to civil engineers.

4.2.1. Evaluation of the specific inner surface

According to the Porod's law, the tail of the SANS curves drops down $\sim Q^{-4}$. After subtracting the scattering background, the Porod region (where $d\Sigma/d\Omega(Q)\sim Q^{-4}$ is fulfilled) is directly observable in the so-called Porod plot ($d\Sigma/d\Omega(Q)\times Q^4$ vs. Q). The Porod region is evident as a horizontal part in this plot. An extrapolation of that plateau, which can be very small or does not exist at all, to $Q=0$ gives the magnitude of the Porod constant K_p as the ordinate intercept. In Fig. 4, the small plateaus of both curves are visible in the Porod plot.

With the help of the Porod plot (see Fig. 4), the determination of the two different Porod constants K_p could be realized. Using the Porod's law, three details of the sample are required: (i) the stoichiometry of the formed C–S–H phase; (ii) their mass density; (iii) their scattering contrast. Using the C–S–H-phase model with the stoichiometry $C_{1.7}SD_{2.1}$ (mass density = 2.23 g/cm^3, scattering length density = 5.018×10^{14} m^{-2}) and the scattering length density of D (heavy water) of 6.339×10^{28} m^{-4}, a scattering contrast u [C–S–D/D] = 1.745×10^{28} m^{-4} was calculated. The scattering contrast is given by the absolute square of the difference of the scattering length densities (scattering object and surrounding medium) [31]. The inner surfaces were calculated and identified as the specific surface area of the C–S–D phase. Here, D stands for D_2O used as mixing water to improve the statistical properties of the scattering signal (see sample preparation). The results, K_p and the specific surface area of C–S–D, are summarized in Table 4. The calculation of the specific surface from the Porod constant is demonstrated in Ref. [28].

At different *w/s* values different pore structures develop, showing, inter alia, different inner surface areas. An increasing *w/s* value results in an increase in the specific inner surface. Recalling the quantitative interpretation of the curves in Fig. 3, the increased number of small particles causes an increase of the total surface. The magnitudes might cause some surprise because typical values of specific surface measured by BET (using nitrogen as adsorbent) are usually in the order of some 10 m^2/g. In one of our previous publications [28], specific surfaces in the order of ~20 m^2/g were calculated from SANS results. This discrepancy can be explained as follows. In the previous work, the Porod plateau appeared in the Q range of about 0.8–1.1 nm^{-1}. The larger values given in Table 4 were measured with a different instrument (V4), and the Porod plateau appeared in

Table 4
Summary of results (via Porod plot)

Number	*w/s*	Porod plot	Calculation results
		Porod constant K_p (cm^{-1} sr^{-1} nm^{-4})	Specific surface area of C–S–D (m^{2}g^{-1})
P6	0.4	1.22 ± 0.07	499 ± 29
P13	0.6	1.48 ± 0.06	605 ± 25

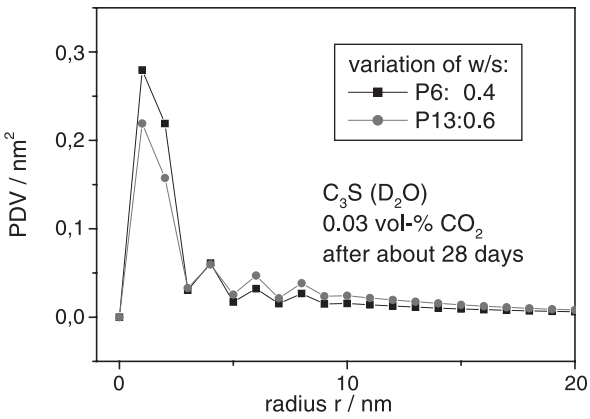

Fig. 5. Volume-weighted particle-size distributions (PDV, plotted in a range of ~0–20 nm).

the Q range of about 3–4 nm^{-1}. The appearance of the Porod plateau at the higher Q range means a better spatial resolution of the measurement in the Porod regime. The surfaces were measured with a smaller etalon, and therefore, the surface determination resulted in higher values. This behavior can be observed for every measuring procedure. The smaller the etalon, the higher the measured magnitude. The discussion prompts a fundamental question in measurement; the measured size (length, area, volume, etc.) can depend on the resolution of the measuring instrument. For example, a measured surface area of a table is nearly independent of the resolution, unless it reaches a spatial resolution in the order of the surface roughness. Therefore, it is principally impossible to determine the correctness of the measured inner surface independently from the method. These discussions must not be interpreted to imply that the Porod procedure for a calculation of specific surfaces is not an exact one. Another possibility to evaluate SANS results is the application of fractal geometry.

An especially interesting situation arises if microstructural objects with fractal behavior exist. According to the aggregation of the very small particles during the hydration processes (for instance as a result of precipitation), an assumption of fractal structures is suggested. Microscopic images support this view [32]. Furthermore, a large variety of SANS and small-angle X-ray scattering (SAXS) data obtained by measurements on hydrating cement pastes have been published. These results indicate that the scattering objects do not obey the Euclidean geometry. The morphology of the agglomerated hydration products (C–S–H phases) emphasizes their description as volume or mass fractals [25,27,33]. The word "mass fractal" is synonymous to the word "volume fractal." Volume fractality describes the spatial scaling behavior (volume). The scaling behavior of the surfaces or interfaces is characterized by the surface fractality [8]. Using the fractal theory, a dependence of the inner surface structure on the *w/s* value can be discussed and explained.

4.2.2. Calculation of particle-size distributions

A size distribution of the scattering objects was calculated by the computer program GIFT [29,30]. This kind of volume-weighted particle-size distribution (PDV) is comparable with the intruded mercury reaching the pore volume inside the sample. MIP reflects the volume, which was penetrated and filled by mercury. So, this size distribution is caused only by the real pores. Hence, the interpretation of MIP results is nonambiguous, but—as already mentioned—it requires completely dried samples, and the method is a destructive one, whereas the SANS patterns result from all scattering objects (pores, particles, etc.) existing in the size range of resolvable structures.

Applying the GIFT routine, the PDV functions were calculated from the total SANS curves (see Fig. 3). For a better discussion, the PDV curve is divided into two ranges of the particle radius r (see Figs. 5 and 6).

The PDV curves were calculated assuming spherically shaped particles in a two-phase system (e.g., solid phase and pores). These assumptions are made for modeling. Recalling the fact that the measuring signal is one dimensional ($d\Sigma/d\Omega(Q)$ vs. Q), the corresponding variable (size of the scattering particles) is one dimensional as well. It is useful to introduce the radius of a sphere as a quantitative parameter. Using this simplification, the much more complex structure of the hydration products (see Fig. 1 and, e.g., Ref. [3]) should always be kept in mind. Irrespective of the different *w/s* values, all PDV curves show a peak at a radius of about 2 nm in Fig. 5. The result is confirmed by the findings of Jennings [34]. In this paper, spherically shaped particles of approximately 2–3 nm are discussed as basic building blocks. It should be mentioned that these SANS results agree with earlier published data on the cement paste microstructure [10,35]. The sample with a lower *w/s* value shows a slightly higher amount of this 2-nm population. Looking at Fig. 6, the use of the higher *w/s* value resulted in an increase of hydration particles in a size range of about 50 nm. This can be explained

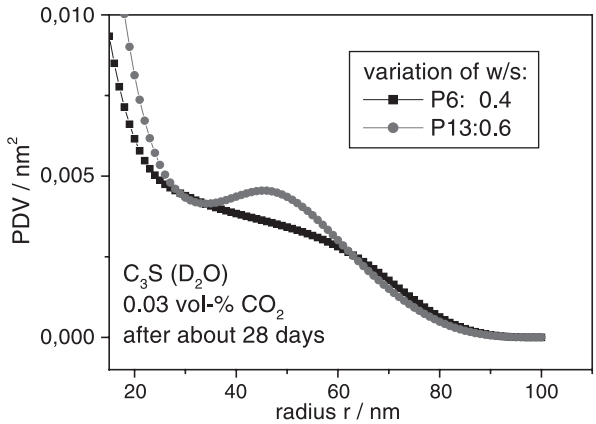

Fig. 6. Volume-weighted particle-size distributions (PDV, plotted in a range of ~20–100 nm).

by the greater distance between the clinker particles at the beginning of hydration. The greater the space available, the larger hydration product particles can be formed.

5. Discussion and conclusions

As demonstrated in this paper, SANS is a useful tool, because it is a nondestructive method and delivers results on a sample volume of about 0.5 cm^3, which can be considered as an average of all resolvable structural details of the whole cement paste. Repeated measurements at the same sample are possible allowing, e.g., the observations of time-dependent changes. However, the evaluation requires models (assumptions). For assumptions regarding the shape of the microstructural objects, direct imaging methods like ESEM can be used. As already pointed out, the obtained information refers only to a part of the cement paste structure, due to the limited spatial resolution of SANS (the resolution can differ between different instruments). It must be emphasized that there is not any method that exists which is able to deliver a complete picture of the total structure. A validation of the quantitative SANS results is impossible because there exists no model for technically relevant macroscopic parameters (strength, durability, permeability,. . .) requiring results of nanometer-sized structural details as input parameters (e.g., specific inner surface). For the same reason, the results obtained via other methods for microstructure investigation (e.g., BET, MIP) cannot be validated either.

SANS measures nanometer-sized structures. This includes the nanometer-sized pores of the total pore system of cement pastes. Peschel [36] has discussed the conditions under which pore water is structured. It was demonstrated that water or an aqueous solution (pore solution) located in pores with diameters smaller than about 6 nm is structured. In this case, water does not completely follow the laws of classical thermodynamics (e.g., shifts in melting, boiling, and triple point) [1]. Hence, the behavior of the pore solution present in such small pores is affected by changes in thermodynamics, which makes understandable that also the solubility of substances is affected. This must be taken into account in the evaluation of PSA results.

It can be concluded from the PSA studies, showing that obviously no ethanolamine was present in the so-called gel water, that the gel water did not act as a solvent. As the gel water evaporates at 105 °C, the bound and free content of a substance, therefore, cannot be determined on the basis of the concentration of this substance found in the expressed pore solution, on the one hand, and the content of vaporizable water, on the other. The fact that the gel water did not act as a solvent seems to support the theory that the gel water is a part of the structure and does not fill pores [21]. This is in contrast to the frost theory, according to which a part of the gel water can be mobile. The frost theory explains the fact that at the beginning of ice formation, the volume contraction of a cement paste sample with a low *w*/*c* value is caused by a movement of water out of the gel pores into larger pores containing already ice [1].

If the frost theory is true and if the gel water does fill pores indeed, it seems not very logical that it did not contain ethanolamine. On the other hand, if the gel water is present as interlayer water of the hydrated cement, it cannot act as a solvent and, therefore, cannot contain any ethanolamine. At any rate, the findings do not provide an answer to this questions because there exist other possible reasons for the absence of ethanolamine in the gel water, too. One possible explanation is that the layer of hydration products covering the cement grains becomes quite dense relatively soon after the onset of hydration. It might be that only water molecules are able to percolate this layer for a long period of time and that ethanolamine molecules get into contact with the reaction zone only for a short time (surface of non-hydrated grains). Therefore, the ethanolamine molecules remain in the capillary pores, in which the expressible pore solution is present. Another possibility might be that the same forces which cause a structured pore solution influence the behavior of this water as a solvent. This thermodynamic explanation cannot be further discussed because the authors are not experts in thermodynamics. However, the authors believe that the findings are of relevance to fundamental mechanisms in general and to the understanding of the nature of the so-called gel water in particular.

Acknowledgements

The work of the second-mentioned author was supported by the Deutsche Forschungsgemeinschaft (DFG) under contract no. Ha2759/3-1 and Ha2759/3-2. He thanks also the IMB of the Universität Leipzig (Prof. G. König and coworkers) and the FIB of the Bauhaus-Universität Weimar (Prof. J. Stark and coworkers) for their collaboration in the experimental work and their helpful discussions. Furthermore, we want to thank the SANS group (HMI) for their help with the SANS experiments. More especially, one author (F.H.) wants to thank Prof. S. Röhling, Leipzig, and Prof. H. Baumbach (Fh-IZFP Saarbrücken) for their kind interest in our work.

References

[1] M. Setzer, Micro ice lens formation, in: M.J. Setzer (Ed.), Proceedings of the 3rd International Bolomey Workshop "Pore Solution in Hardened Cement Paste", University of Essen, June 1998, AEDIFICATIO Publishers, Freiburg, 2000, pp. 89–112.

[2] S. Röhling, H. Eifert, R. Kaden, Betonbau. Planung und Ausführung, in: S. Röhling, H. Eifert, R. Kaden (Eds.), Verlag Bauwesen, Berlin, 2000.

[3] J. Stark, B. Wicht, Anorganische Bindemittel Zement-Kalk-Spezielle Bindemittel, Schriften der Bauhaus-Universität, Fakultät Bauingenieurwesen, FIB-F.A. Finger-Institut für Baustoffkunde Weimar, 1998.

[4] R.S. Barneyback Jr., S. Diamond, Expression and analysis of pore fluids from hardened cement pastes and mortars, Cement and Concrete Research 11 (1981) 279–285.
[5] G. Kostorz, Small-angle scattering and its application to materials science, in: G. Kostorz (Ed.), Treatise on Materials Science and Technology, Academic Press, London, 15 (1979) 227–259.
[6] A. Guinier, G. Fournet, Small-Angle Scattering of X-rays, Wiley, New York, 1955.
[7] O. Glatter, O. Kratky, Small-Angle X-ray Scattering, Academic Press, London, 1982.
[8] F. Häußler, S. Palzer, A. Eckart, Nondestructive microstructural investigations on hydrating cement paste and tricalcium silicate by small angle neutron scattering, Leipzig Annual Civil Engineering Report, (1999) 47–64.
[9] F. Häußler, H. Hermann, A. Heinemann, S. Palzer, A. Eckart, Mikrostrukturuntersuchungen an hydratisierendem C_3S und PZ mittels Neutronenkleinwinkelstreuung (Vortrag), Tagungsbericht- Band 1, 14. Internationale Baustofftagung IBAUSIL, Bauhaus-Universität Weimar, 20.-23.09.2000, pp. 1-0433–1-0442.
[10] A.J. Allen, R.C. Oberthur, D. Pearson, P. Schofield, C.R. Wilding, Development of the fine porosity and gel structure of hydrating cement systems, Philosophical Magazine, B 56 (1987) 263–288.
[11] F. Häußler, H. Baumbach, M. Kröning, Non-destructive characterization of materials with neutron experiments at the pulsed reactor IBR-2, Nondestructive Characterization of Materials 6 (1994) 435–444.
[12] S. Röhling, M. Nietner, Anwendung eines strukturorientierten Modells zur Berechnung der Festigkeitsentwicklung von Zementbeton, Betontechnik 9 (1988) 52–53.
[13] S. Diamond, Mercury porosimetry—an inappropriate method for the measurement of pore size distributions in cement-based materials, Cem. Concr. Res. 30 (1) (2000) 1517–1525.
[14] E. Brunauer, P.H. Emmett, E. Teller, Adsorption of gases in mulitmolecular layers, Journal of the American Chemical Society 60 (1938) 309–319.
[15] F. Häußler, Neutronenkleinwinkelstreuung- Ein Beitrag zur mikrostrukturellen Aufklärung des hydratisierenden Zementsteins (invited talk), Baustoff-Kolloquium, F.A. Finger-Institut für Baustoffkunde (Prof. J. Stark) der Bauhaus-Universität Weimar, 06.04.2001.
[16] J. Tritthart, Chloride binding in cement: I. Investigations to determine the composition of pore water in hardened cement, Cem. Concr. Res. 19 (1989) 586–594.
[17] T.C. King, C.M. Dobson, S.A. Rodger, Hydration of tricalcium silicate with D_2O, Journal of Material Science Letters 7 (1988) 861–863.
[18] J.J. Thomas, H.M. Jennings, A.J. Allen, The surface area of cement paste as measured by neutron scattering: evidence for two C–S–H morphologies, Cem. Concr. Res. 28 (6) (1998) 897–905.
[19] F. Häußler, S. Palzer, A. Eckart, Nanostructural investigations on carbonation of hydrating tricalcium silicate by small angle neutron scattering, Leipzig Annual Civil Engineering Report, (2000) 181–196.
[20] T.C. Powers, T.L. Brownyard, Studies of the physical properties of hardened Portland cement paste, Proceedings of the American Concrete Institute 43 (1947) 669.
[21] R.F. Feldman, P.J. Sereda, A new model for hydrated Portland cement and its practical implications, Engineering Journal (1970) 53–59.
[22] J.J. Beaudoin, P.W. Brown, The structure of hardened cement paste, Proceedings of the 9th Intern. Congr. Chem. Cem. vol. 1, National Council for Cement and Building Materials (NCB), 1993, pp. 485–525.
[23] W. Wieker, C. Hübert, D. Heidemann, Recent results of solid-state NMR investigations and their possibilities of use in cement chemistry, Xth Int. Congr. In Cement Chemistry Gothenburg 1997 (Sweden), Plen 2, 24 pp, ISBN 91-630-54-95-7.
[24] G. Best, A. Cross, H. Peemoeller, M.M. Pintar, R. Blinc, Distribution of pores sizes in white cement paste from proton NMR spin-lattice relaxation, Advances in Cement Research 8 (1996) 163.
[25] A. Heinemann, et al., Fractal microstructures in hydrating cement paste, Journal of Material Science Letters 18 (1999) 1413–1416.
[26] S.A. FitzGerald, D.A. Neumann, J.J. Rush, D.P. Bentz, R.A. Livingston, In situ quasi-elastic neutron scattering study of the hydration of tricalcium silicate, Chemistry of Materials 10 (1998) 397–402.
[27] A.J. Allen, R.A. Livingston, Relationship between differences in silica fume additives and fine-scale microstructural evolution in cement based materials, Advances in Cement-Based Materials 8 (1998) 118–131.
[28] F. Häußler, M. Hempel, H. Baumbach, J. Tritthart, Nanostructural investigations of hydrating cement pastes produced from cement with different fineness levels, Advances in Cement Research 13 (2001) 65–73.
[29] B. Weyerich, J. Brunner-Popela, O. Glatter, Small-angle scattering of interacting particles: II. Generalized indirect Fourier transformation under consideration of the effective structure factor for polydisperse systems, Journal of Applied Crystallography 32 (1999) 197–209.
[30] O. Glatter, A new method for the evaluation of small-angle scattering data, Journal of Applied Crystallography 10 (1977) 415–421.
[31] J.J. Thomas, H.M. Jenning, A.J. Allen, Determination of the neutron scattering contrast of hydrated Portland cement paste using H_2O/D_2O exchange, Advances in Cement-Based Materials 7 (3) (1998) 119–122.
[32] M. Langenfeld, J. Stark, Der Einfluss von Verzögerern auf die frühe Hydratation von Portlandzementklinkerphasen, dargestellt im ESEM-FEG, Thesis, Beiträge zur Baustofforschung, Wissenschaftliche Zeitschrift der Bauhaus-Universität, 44 (1998) 1/2, S. 83–90.
[33] M. Kriechbaum, G. Degovics, P. Laggner, J. Tritthart, Investigations on cement pastes by small-angle X-ray scattering and BET: the relevance of fractal geometry, Advances in Cement Research 6 (1994) 93–101.
[34] H.M. Jennings, A model for the microstructure of calcium silicate hydrate in cement paste, Cem. Concr. Res. 30 (1) (2000) 101–116.
[35] D. Pearson, A. Allen, C.G. Windsor, N.McN. Alford, D.D. Double, An investigation on the nature of porosity in hardened cement pastes using small angle neutron scattering, Journal of Materials Science 18 (1983) 430–438.
[36] G. Peschel, Disjoining forces in pore water, in: M.J. Setzer (Ed.), Proceedings of the 3rd International Bolomey Workshop Pore Solution in Hardened Cement Paste, University of Essen, June 1998, AEDIFICATIO Publishers, Freiburg, 2000, pp. 3–25.